

Inorganic, Monovalent Cations Compete with Agonists for the Transmitter Binding Site of Nicotinic Acetylcholine Receptors

Gustav Akk and Anthony Auerbach*

Department of Biophysical Sciences, State University of New York, Buffalo, New York 14214 USA

ABSTRACT The properties of adult mouse recombinant nicotinic acetylcholine receptors activated by acetylcholine (ACh⁺) or tetramethylammonium (TMA⁺) were examined at the single-channel level. The midpoint of the dose-response curve depended on the type of monovalent cation present in the extracellular solution. The shifts in the midpoint were apparent with both inward and outward currents, suggesting that the salient interaction is with the extracellular domain of the receptor. Kinetic modeling was used to estimate the rate constants for agonist binding and channel gating in both wild-type and mutant receptors exposed to Na⁺, K⁺, or Cs⁺. The results indicate that in adult receptors, the two binding sites have the same equilibrium dissociation constant for agonists. The agonist association rate constant was influenced by the ionic composition of the extracellular solution whereas the rate constants for agonist dissociation, channel opening, and channel closing were not. In low-ionic-strength solutions the apparent association rate constant increased in a manner that suggests that inorganic cations are competitive inhibitors of ACh⁺ binding. There was no evidence of an electrostatic potential at the transmitter binding site. The equilibrium dissociation constants for inorganic ions (Na⁺, 151 mM; K⁺, 92 mM; Cs⁺, 38 mM) and agonists (TMA⁺, 0.5 mM) indicate that the transmitter binding site is hydrophobic. Under physiological conditions, about half of the binding sites in resting receptors are occupied by Na⁺.

INTRODUCTION

Nicotinic acetylcholine receptors (AChRs) are synaptic ion channels composed of five homologous subunits that are activated by small, cationic ligands such as acetylcholine (ACh⁺) and tetramethylammonium (TMA⁺) (del Castillo and Katz, 1957; Marshall et al., 1991; Zhang et al., 1995). Each receptor has two agonist binding sites that are bathed by the extracellular solution (Unwin, 1993). Agonists bind to these sites and cause the pore domain of the protein to change from a "closed" structure that precludes ion permeation to an "open" one that allows monovalent cations to readily pass.

In physiological solutions, many cationic agonists are effective at micromolar concentrations. TMA⁺ associates with embryonic-type AChR more slowly than ACh⁺, but dissociates at about the same rate (Zhang et al., 1995). Because TMA⁺ is the smaller ligand, this suggests that factors other than ligand size determine the affinity of the receptor for an agonist. Inorganic, monovalent cations are smaller than ACh⁺ and TMA⁺, and we wanted to determine the extent to which physiological concentrations of Na⁺ and K⁺ might influence the agonist binding and activation properties of resting AChR. The results of single-channel analyses indicate that physiological ions are competitive inhibitors of ACh⁺ binding. The sequence of equilibrium dissociation constants of the inhibitors is Na⁺ > K⁺ > Cs⁺

> TMA⁺, which suggests that the AChR transmitter binding site is hydrophobic.

MATERIALS AND METHODS

Experimental preparation

cDNA clones of wild-type mouse α -, β -, δ -, and ϵ -subunits were constructed in either pRBG4 (Sine, 1993) or pcDNAlII (Invitrogen, San Diego, CA). Mutant clones α D200N and α G153S were generously provided by Dr. Steven Sine (Mayo Foundation, Rochester, MN). Human embryonic kidney (HEK) 293 cells were transiently transfected by calcium phosphate precipitation (Ausubel et al., 1992). A total of 3.6 μ g of DNA/35-mm culture dish in the ratio 2:1:1:1 (α : β : δ : ϵ) was used. Twenty-four hours after the start of transfection the medium was changed, and 48 h later electrophysiological recordings were started.

Electrophysiology and kinetic analysis

The bath solution was Dulbecco's PBS (in mM): 137 NaCl, 0.9 CaCl₂, 2.7 KCl, 1.5 KH₂PO₄, 0.5 MgCl₂, 6.6 Na₂HPO₄, pH 7.3. The pipette solution was buffered to pH 7.4 with 10 mM HEPES and contained, in addition (in mM), {115 NaCl, 1 CaCl₂}, or {142 KCl, 1.8 CaCl₂, 1.7 MgCl₂, 5.4 NaCl}, or {142 CsCl, 1.8 CaCl₂, 1.7 MgCl₂, 5.4 NaCl}. In experiments at low ionic strength, the pipette solution contained 1.8 CaCl₂, 1.7 MgCl₂, 5.4 NaCl, plus varying amounts of KCl. In experiments with ionic mixtures, the NaCl and CsCl pipette solutions were mixed on a volume basis. The interior of the patch pipette was typically held at +70 mV; assuming a reversal potential of 0 mV and a conductance of 70 pS, we estimate that the membrane potential was \sim -100 mV. The temperature was 22°C. The pipette contained the indicated concentration of ACh⁺ or TMA⁺. All recordings were obtained in the cell-attached configuration (Hamill et al., 1981).

Currents were recorded on an Axopatch 1B amplifier, low-pass filtered at 20 kHz (8-pole Bessel) and stored on videotape in digital format (Instrutech VR-10). For single-channel kinetic analysis, the current record was transferred to a PC computer via a digital interface (Instrutech VR111) at a sampling frequency of 94 kHz. Clusters of current arising from individual receptors were elicited by high ACh concentrations (Sakmann et al., 1980). To identify clusters, the data were digitally filtered (Gaussian

Received for publication 3 November 1995 and in final form 10 February 1996.

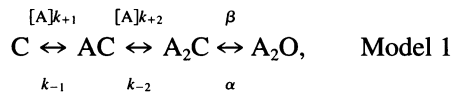
Address reprint requests to Dr. Anthony Auerbach, Department of Biophysical Sciences, SUNY Buffalo, 118 Cary Hall, Buffalo, NY 14214. Tel.: 716-829-2435; Fax: 716-829-2415; E-mail: auerbach@xenopus.med.buffalo.edu.

© 1996 by the Biophysical Society

0006-3495/96/06/2652/07 \$2.00

filter, half-power frequency = 2 kHz) and detected with a half-amplitude criterion. Clusters were defined as a series of openings separated by closed intervals shorter than some critical duration (τ_{crit} , the value of which depended on the type of receptor and concentration of agonist). Once defined, the time constant of the longest closed-interval component within clusters was measured, and further analyses proceeded only if this time constant was at least five times shorter than τ_{crit} . Next, an apparently homogeneous population of clusters was selected with regard to mean amplitude, open duration, and closed duration (see Auerbach, 1993). After rejection of clusters with multiple open channels, approximately 90% of all clusters were selected by these criteria for further analysis. The selected clusters (typically, 20 per patch) were extracted at full bandwidth and were again idealized with a half-amplitude method after low-pass filtering (typically, at a half-power frequency of 7 kHz). The intracluster open and closed durations were obtained by fitting sums of exponentials to interval duration histograms. The open and closed durations reported in the text are the slowest component of these distributions. The effective closing and opening rates (β') are the inverses of the open and closed durations, respectively. The β' versus concentration (A) curves were fitted by the Hill equation to estimate the maximum opening rate (β): $\beta' = \beta/(1 + (K/A)^n)$.

Rate constants of the activation reaction were estimated using an interval maximum likelihood method that employed a correction for missed events (Horn and Lange, 1983; Roux and Sauve, 1985; Qin et al., 1996). The following kinetic scheme (Magleby and Stevens, 1972; Colquhoun and Hawkes, 1977) was used:



where A is the concentration of agonist, C is a closed receptor, O is an open receptor, k_{+1} and k_{+2} are the agonist association rate constants, k_{-1} and k_{-2} are the agonist dissociation rate constants, β is the channel opening rate constant, and α is the channel closing rate constant.

Idealized currents from several patches through a range of agonist concentration were combined. An approximately equal number of intervals from each concentration (typically, 2000) was used. After fitting, error limits were estimated as 0.5 likelihood intervals (Colquhoun and Sigworth, 1983). Interval duration histograms and dose-response curves were calculated from the optimal parameters for comparison with the experimental data. α G153S receptors were activated by 100 nM ACh⁺, and bursts of current, defined as openings separated by closures less than 1 ms in duration, were analyzed. In kinetic analyses of currents at low ionic strengths (Fig. 3 B), the channel opening rate constant was constrained to be 60,000 s⁻¹ and the ACh dissociation rate constant was constrained to be 17,000 s⁻¹.

Binding site equivalence

According to model 1, the probability of being open (P_{open}) versus the concentration curve is described by

$$P_{\text{open}} = ((K_{d1}K_{d2}/A^2\Theta) + (K_{d2}/A\Theta) + 1/\Theta + 1)^{-1}, \quad (1)$$

where A is the concentration of agonist, K_{d1} and K_{d2} are the equilibrium dissociation constants of the two binding sites, and Θ is the gating equilibrium constant (β/α). If the two binding sites are equivalent, then according to model 1, k_{+2} is the agonist association rate constant to a single site, k_{-1} is the agonist dissociation rate constant from a single site, and the equilibrium dissociation constant ($K_d = k_{-1}/k_{+2}$) can be estimated by fitting the dose-response curves to

$$P_{\text{open}} = (K_d^2/\Theta A^2 + K_d/\Theta A + 1/\Theta + 1)^{-1}. \quad (2)$$

The P_{open} versus concentration curves for ACh⁺- and TMA⁺-activated receptors were fitted by Eqs. 2 and 1. The optimal parameters using Eq. 2 (equal binding sites) are shown in Table 1, with the following χ^2 values: ACh⁺, $\chi^2 = 1.27 \times 10^{-3}$; TMA⁺, $\chi^2 = 3.65 \times 10^{-3}$. The P_{open} curves

TABLE 1 Equilibrium constants of wild-type AChR activation in different salts

	K_d (μM)		Θ	
	k_{-}/k_{+}	P_{open}	β/α	P_{open}
ACh ⁺ , Na ⁺	99	102 ± 39	53	47 ± 30
K ⁺	162	164 ± 73	45	43 ± 32
Cs ⁺	200	268 ± 72	24	34 ± 14
TMA ⁺ , Na ⁺	829	1134 ± 432	5.4	8.0 ± 3.5

Equilibrium constants were estimated from either rate constants estimated by single-channel kinetic analysis (k_{-}/k_{+} or β/α ; see Table 2), or from P_{open} curves by fitting Eq. 2. Wild-type receptors were activated by 5–200 μM ACh⁺ or 200–2000 μM TMA⁺.

were also fitted by Eq. 1 (without the constraint of equal binding sites). The errors of the parameter estimates became large (ACh⁺: $K_{d1} = 55 \pm 69$, $K_{d2} = 178 \pm 413$, $\Theta = 44 \pm 65$; TMA⁺: $K_{d1} = 836 \pm 3807$, $K_{d2} = 3304 \pm 1421$, $\Theta = 8.2 \pm 8$), and the χ^2 values did not change significantly compared to the constrained fit. Furthermore, the optimal estimates were such that $K_{d2} \approx 4K_{d1}$, which is expected if the binding sites are equal. In addition, the rate constants obtained from single-channel analysis assuming equal binding adequately describe the open- and closed-interval duration histograms, the effective opening rate curves, and dose-response properties of adult-type AChR. Removing the constraint that the binding sites are equal did not significantly increase the log likelihood of the fit of the single-channel data. Thus neither the P_{open} nor the single-channel analyses warrant a conclusion that the binding sites of adult-type ($\alpha_2\beta\delta\epsilon$) AChR are different, as they are in receptors expressed with a γ -subunit (Sine et al., 1990; Zhang et al., 1995; Unwin, manuscript in preparation).

RESULTS

Fig. 1 shows the dose-response properties of adult-type receptors activated by ACh⁺ in different ionic environments. The concentration of ACh⁺ at which the probability that a receptor is open (P_{open}) is half-maximal (EC_{50}) is higher in the presence of Cs⁺ (46 μM) or K⁺ (28 μM) compared to Na⁺ (16 μM). The P_{open} is determined by the durations of both open and/or closed intervals. Fig. 1 D shows that only the closed-interval durations change with the ionic environment. Closed intervals are longer-lived (i.e., receptors appear to open more slowly) in the presence of Cs⁺ compared to Na⁺.

Na⁺, K⁺, and Cs⁺ permeate the AChR pore (Adams et al., 1980), and it was possible that interactions of ions within the pore influence the dose-response properties of the receptor (Gage and Van Helden, 1979). We therefore examined the effects of the ionic composition of the extracellular solution at depolarized potentials where, in cell-attached patches, the ions that make up the outward current (mostly K⁺) are essentially independent of the composition of the pipette solution. Fig. 1 B shows that the shifts in P_{open} and closed-interval duration are similar at both depolarized and hyperpolarized potentials. These results suggest that interactions of ions with the extracellular domain of the receptor, rather than the pore, determine the duration of closed intervals.

Next, we determined whether the observed increase in closed-interval duration (the slower apparent opening rate) in different ionic environments arises from alterations in the

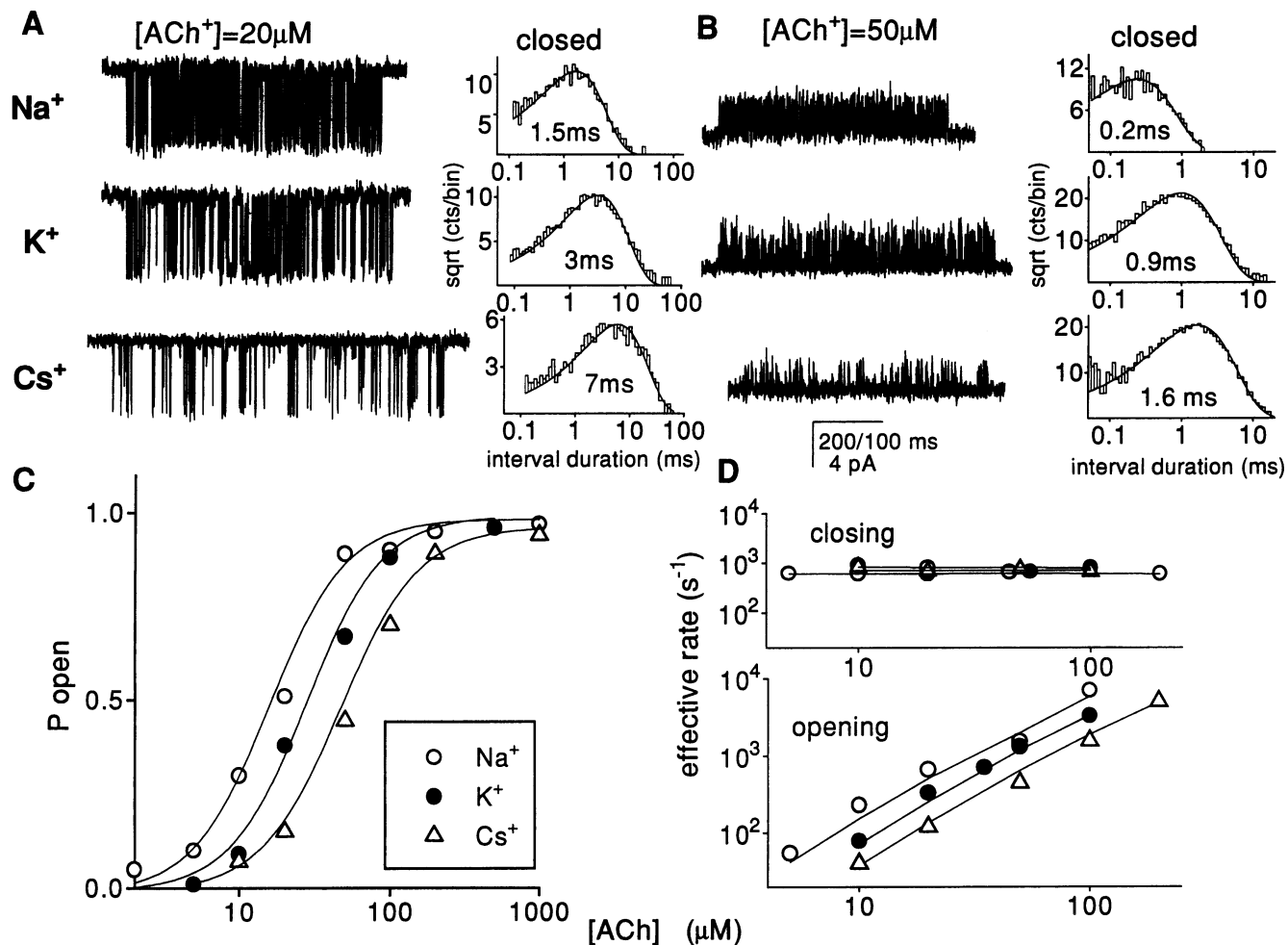


FIGURE 1 Activation properties of adult, wild-type mouse AChR in different ionic environments. (A) Example clusters and closed interval duration histograms from receptors exposed to external Na^+ (top), K^+ (middle), or Cs^+ (bottom). The membrane potential was -100 mV (inward current is down). (B) Depolarization of the patch to $+40$ mV elicits outward currents. The effect of the ionic environment on the duration of closed intervals within clusters does not depend on the direction of the current. (C) Dose-response curves in different ionic environments. The EC_{50} increases from $16 \mu M$ in Na^+ , to $28 \mu M$ in K^+ , to $46 \mu M$ in Cs^+ . Each symbol is from a single patch. The P_{open} values are the means computed from 10 to 48 (mean = 21) clusters per patch. The average SD of the P_{open} was 0.05. (D) Effective opening and closing rates in different ionic environments. Only the effective opening rate (i.e., the inverse of the slowest component of the intracluster closed interval duration distribution) depends on the extracellular ions. Each value is the inverse of the time constant of the slowest component of the intracluster open or closed interval duration histogram. The error limits of these time constants were 4–9% of the optima. In both C and D the lines are computed from the rate constants in Table 2.

agonist binding and/or channel gating processes. Wild-type AChRs open very rapidly ($\sim 60,000 s^{-1}$; Sine et al., 1995), too fast for us to clearly determine whether the extracellular ionic environment influences this rate constant. A mutant AChR in which an aspartate at position 200 of the α -subunit is changed to an asparagine ($\alpha D200N$) has a much slower opening rate constant (O'Leary and White, 1992; Akk et al., manuscript in preparation), allowing us to more readily determine whether the ionic environment influences this value in the mutant receptor. Fig. 2 A shows that the EC_{50} s for $\alpha D200N$ receptors are shifted by the ionic environment to an extent similar to those of wild-type receptors. At very high ACh^+ concentrations, binding is saturated and the apparent opening rate (the inverse of the closed interval duration) is equal to the intrinsic channel opening rate

constant, β (see model 1, Materials and Methods). Fig. 2 B shows that the opening rate constant of $\alpha D200N$ receptors, however, is similar in the presence of Na^+ ($542 s^{-1}$), K^+ ($614 s^{-1}$), and Cs^+ ($629 s^{-1}$).

$\alpha D200N$ receptors open ~ 100 times more slowly than the wild type, and it was possible that such slowly opening receptors are not influenced by the composition of the ionic environment. We therefore examined the effects of extracellular ions on a mutant ACh receptor that opens rapidly. A glycine-to-serine substitution at position 153 of the α -subunit ($\alpha G153S$) yields a receptor that opens at $\sim 50,000 s^{-1}$ but gives rise to currents that are relatively easy to analyze because of a greatly slowed agonist dissociation rate constant (Sine et al., 1995). The effects of the ionic environment with $\alpha G153S$ receptors (Table 2) were similar to those

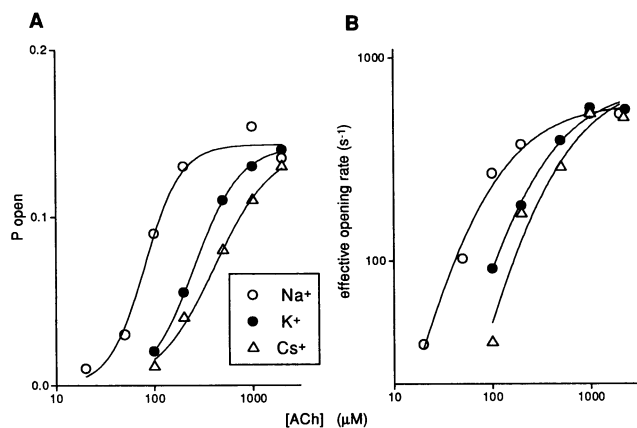


FIGURE 2 Mutant AChR α D200N. (A) Dose-response curves in different ionic environments. The EC_{50} increases from 89 μ M in Na^+ , to 249 μ M in K^+ , to 414 μ M in Cs^+ . Each symbol is from a single patch. The P_{open} values are the means computed from 4 to 44 (mean = 9) clusters per patch. The average SD of the P_{open} was 0.02. (B) The effective opening rate versus [ACh]. At high concentrations the effective opening rate reflects only the channel opening rate constant, which saturates at the same level for all ions. The α D200N opening rate constant does not change with the ionic environment. Each symbol is from a single patch. Each β' value is the inverse of the time constant of the slowest component of the intracluster closed interval duration histogram. The error limits of this time constant were 3–5% of the optima.

for α D200N receptors. The opening rate constant and the ACh^+ dissociation rate constant were not substantially influenced by the ionic composition of the extracellular solution. Together, the results with these mutants suggest that the ionic environment does not influence channel gating. We therefore conclude that the change in the dose-response and apparent opening rate curves in the presence of different ions arises from a change in the receptor's agonist binding properties.

To further study these changes in agonist binding we analyzed single-channel currents according to model 1, with the constraint that the two binding sites are equivalent. The results of fitting the dose-response curves using Eq. 2 are shown in Table 1. The gating equilibrium constant is similar in Na^+ and K^+ , but the equilibrium dissociation constant for ACh^+ is ~ 1.6 -fold lower in K^+ , and 2.7-fold lower in Cs^+ , compared to Na^+ .

Single-channel kinetic modeling was used to determine whether the changes in the apparent K_d in the presence of different ions arise from changes in the rate constants of agonist association and/or dissociation. The results are shown in Table 2. The extracellular ionic environment influences the ACh^+ association rate constant but has little or no effect on the dissociation rate constant. ACh^+ appears to bind to receptors ~ 2.6 times more slowly in the presence of Cs^+ compared to Na^+ .

One mechanism by which the apparent association rate constant can be slowed is competitive inhibition. If a single inorganic monovalent cation competes with ACh^+ for the activation site, then the apparent association rate constant

(k_+) will be slowed in proportion to the concentration of the competing ion ([i]) according to

$$k_+ = k_+^*/(1 + [i]/K_i), \quad (3)$$

where k_+^* is the association rate constant in pure water, and K_i is the equilibrium dissociation constant for the competing ion.

The influence of a competitive ligand is reduced by lowering its concentration, or in this case, by working in low-ionic-strength solutions. Fig. 3 A shows that as the concentration of K^+ is lowered (from 142 mM to 3 mM), the P_{open} of clusters (elicited by 10 μ M ACh) increases. This increase can be traced to a reduction in the duration of closed intervals, i.e., a faster apparent opening rate. Fig. 3 B shows the result of using single-channel kinetic analysis to estimate the apparent k_+ values in K^+ solutions of differing ionic strengths. Fitting these values by Eq. 3 produces the result $k_+^* = 2.6 \pm 0.1 \times 10^8 \text{ M}^{-1} \text{ s}^{-1}$ and $K_i = 92 \pm 18 \text{ mM}$ for K^+ . In the presence of 150 mM KCl, the apparent ACh^+ association rate constant is about 2.5 times slower than it is in pure water because of competition between ACh^+ and K^+ . The calculated K_d for ACh^+ in pure water is 60 μ M, i.e., the activation site of resting AChR prefers ACh^+ over K^+ by a factor of about 1500.

In experiments at low ionic strengths, the effectiveness of any negative surface charges near the transmitter binding site will increase. We therefore explored the possibility that the observed increase in the apparent association rate constant of ACh^+ was caused by such a mechanism rather than by competitive inhibition by ions. k_+ was measured in mixtures of NaCl and CsCl, where the ionic strength of the solution was nearly constant. In the absence of a surface charge effect, the apparent association rate constant will change with the concentration of the competing ions according to

$$k_+ = k_+^*/(1 + [Na^+]/K_{i,Na} + [Cs^+]/K_{i,Cs}), \quad (4)$$

where the association rate constant for ACh^+ in pure water, $k_+^* = 2.6 \pm 0.1 \times 10^8 \text{ M}^{-1} \text{ s}^{-1}$, was determined from the experiments at low ionic strength. The results are shown in Fig. 3 C. In mixtures of Na^+ and Cs^+ , the apparent association rate constant was in close agreement with the values predicted from Eq. 4, i.e., from ionic competition alone. We conclude that that surface charges do not significantly influence the ACh^+ association rate constant, and that inorganic ions indeed compete with ACh^+ for the transmitter binding site.

Finally, we used single-channel kinetic analysis to determine the association and dissociation rate constants in adult-type AChR for TMA^+ (Fig. 4 and Table 2). As was the case with embryonic-type AChR (Zhang et al., 1995), TMA^+ binds to receptors ~ 10 times more slowly than does ACh^+ but escapes at about the same rate. As a result, the equilibrium dissociation constant for TMA^+ is ~ 10 times higher than for ACh^+ . In addition, TMA^+ -activated receptors open ~ 10 times more slowly than do receptors activated by ACh,

TABLE 2 Activation rate constants of wild-type and α G153S AChR in different ionic environments

	k_+ ($\times 10^{-8}$ M $^{-1}$ s $^{-1}$)	k_- (s $^{-1}$)	β (s $^{-1}$)	α (s $^{-1}$)
Wild-type				
ACh $^+$				
Na $^+$	1.69 \pm 0.01	16,540 \pm 711	—	1,132 \pm 22
K $^+$	1.11 \pm 0.02	18,020 \pm 422	—	1,321 \pm 15
Cs $^+$	0.65 \pm 0.03	13,047 \pm 714	—	2,530 \pm 64
TMA $^+$				
Na $^+$	0.15 \pm 0.01	12,249 \pm 1262	8,156 \pm 382	1,508 \pm 205
α G153S				
ACh $^+$				
Na $^+$	—	929 \pm 362	46,043 \pm 8304	567 \pm 69
K $^+$	—	989 \pm 95	48,584 \pm 1388	726 \pm 20
Cs $^+$	—	1,720 \pm 371	55,897 \pm 4899	886 \pm 78

For each ionic environment >3000 intervals from >4 patches (wild type), or >4500 intervals from 3 patches (α G153S) were analyzed. The opening rate constant for ACh $^+$ -activated wild-type receptors was constrained to be 60,000 s $^{-1}$. Rate constants were estimated from the durations of idealized single-channel intracuster open and closed intervals using model 1, with a maximum likelihood method that contained a correction for missed events. Error limits on the rate constants are 0.5 likelihood intervals obtained by bisection. With adult-type AChR, the use of kinetic models that allowed binding sites with different association and dissociation rate constants did not result in a significantly better fit.

but the two close at about the same rate. The net effect of these binding and gating differences is a \sim 36-fold higher EC $_{50}$ for AChR activated by TMA $^+$ compared to ACh $^+$.

The ACh $^+$ activation rate constants predict the following average parameters for the decay of the adult mouse end-plate current (epc). An AChR channel opens 1.8 times, with each opening lasting 880 μ s, to produce an epc decay time constant (at -100 mV, 22°C) of 1.6 ms. Both the channel closing rate constant and the agonist dissociation rate constant determine the epc lifetime.

DISCUSSION

The central conclusion of these experiments is that physiological concentrations of monovalent cations competitively inhibit transmitter binding to resting mouse nicotinic ACh receptors. Almost 20 years ago Gibson et al. (1977) concluded that series I monovalent cations were competitive inhibitors of ACh binding to desensitized, detergent-solubilized *Torpedo* ACh receptors. In their experiments, the K_i for K $^+$ was \sim 270 mM, or \sim 3 times larger than in our experiments. Desensitized receptors have a >1000-fold higher affinity for ACh $^+$ than do resting receptors (Sine et al., 1994). It is possible that the greater $K_{i,K}$ in the experiments with *Torpedo* receptors reflects the character of the desensitized (compared to the resting) binding site.

The conclusion that ions compete with agonists for the transmitter binding site does not rest on model-based kinetic analyses. The mean closed times of wild-type receptors vary with the ion, but the mean open times do not (Fig. 1 D), suggesting that binding, rather than gating, is altered by the ions. This conclusion was confirmed by the direct measurement of opening rate constants (with different ions) of a slowly opening, mutant receptor (Fig. 2 B). In addition, the effect of the ionic environment is unchanged at depolarized potentials (Fig. 1 B), suggesting that the salient interaction is at the binding site rather than the pore. Thus, even without

kinetic modeling of single-channel currents, the data suggest that the ions compete with ACh for the transmitter binding site.

Because of this competition, in 150 mM NaCl the apparent ACh $^+$ and TMA $^+$ association rate constants measured in physiological solutions are about half their values in pure water. Thus, an ACh dose-response curve obtained in distilled water would have an EC $_{50}$ value of \sim 10 μ M, compared to \sim 20 μ M in 150 mM NaCl. Similarly, an equilibrium dissociation constant determined from competitive binding assays will be influenced by the composition of the ionic environment. In addition, the amplitude of a synaptic current might be reduced, and its rise time could be slowed, by the competitive binding of physiological cations.

The equilibrium selectivity of the AChR transmitter binding site for monovalent cations is given in Table 3. This series is characteristic of a hydrophobic site in which dehydration of the ion is the predominant factor that determines the equilibrium occupancy of the site (Hille, 1992). The relatively greater difference in K_d between K $^+$ and ACh $^+$ in desensitized *Torpedo* (Gibson et al., 1977) compared to resting mouse receptors suggests that the hydrophobicity of the binding site might increase upon desensitization.

Our results indicate that the occupancy of a site or sites by an inorganic ion prevents the access of ACh $^+$ to its docking site, but we do not know whether the "site" is a localized or a distributed structure (Unwin, 1993). For example, acetylcholinesterase has a binding gorge that is lined by aromatic residues (Sussman et al., 1991), and the non-polar microenvironment of this structure might favor the equilibrium occupancy of "hydrophobic" cations (ACh $^+$ and TMA $^+$) over "hard" cations (Na $^+$ and K $^+$).

The ionic species in the extracellular solution influence the dose-response profile and activation kinetics of AChR via competitive inhibition at the transmitter binding site. Mutations

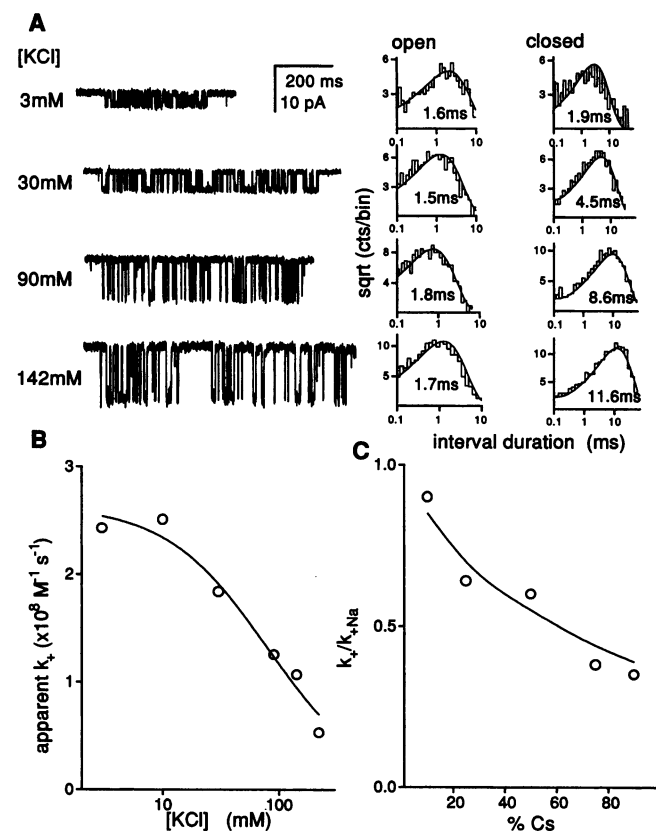


FIGURE 3 Wild-type receptors in low-ionic-strength solutions. (A) Example clusters and closed interval duration histograms at $10 \mu\text{M}$ ACh^+ with solutions of different ionic strength in the pipette. Only the [KCl] was varied. The membrane potential was -150 mV . Cluster P_{open} decreases with increasing ionic strength because closed intervals become longer. Intervals from n patches at different ACh concentrations ($5\text{--}100 \mu\text{M}$) were combined at each K^+ concentration (3 mM , $n = 2$, 10 mM , $n = 4$; 30 mM , $n = 4$; 90 mM , $n = 1$; 142 mM , $n = 4$; 220 mM , $n = 1$). For each symbol, 6 to 59 clusters (mean = 27) containing 2,598 to 16,420 (mean = 6,390) open and closed dwells were analyzed by a maximum interval likelihood method. (B) The apparent association rate constant, estimated by single-channel kinetic analysis, increases as the [KCl] decreases. The line is fitted by Eq. 3, with $k_+^* = 2.6 \times 10^8 \text{ M}^{-1} \text{ s}^{-1}$ and $K_{i,K} = 92 \text{ mM}$. (C) The apparent association rate constant changes with the ionic environment at constant ionic strength. Na^+ and Cs^+ solutions (see Materials and Methods for exact compositions) were mixed at the ratios indicated by the x axis. The rate constant determined from single-channel kinetic analysis has been normalized by its value in pure Na^+ solution. Each symbol is from one patch, with from 8 to 16 clusters (mean = 13) and 1015 to 2308 (mean = 1714) intracuster intervals. The error limits, estimated from 0.5 likelihood intervals on k_+ , were 2–3% of the mean. The line is drawn according to Eq. 4 using $k_+^* = 2.6 \times 10^8 \text{ M}^{-1} \text{ s}^{-1}$, $K_{i,\text{Na}} = 92 \text{ mM}$, and $K_{i,\text{Cs}} = 38 \text{ mM}$. The good agreement between the experimental k_+ values and those calculated directly (not fit) from this equation indicates that ion competition, rather than surface potential, influences the apparent association rate constant.

to the AChR binding site region have been shown to shift the midpoints of dose-response and binding curves (Tomaselli et al., 1991; O'Leary and White, 1992; Sine et al., 1994) or to reduce the apparent association rate constant (Aylwin and White, 1994; Chen et al., 1995). It is possible that such shifts

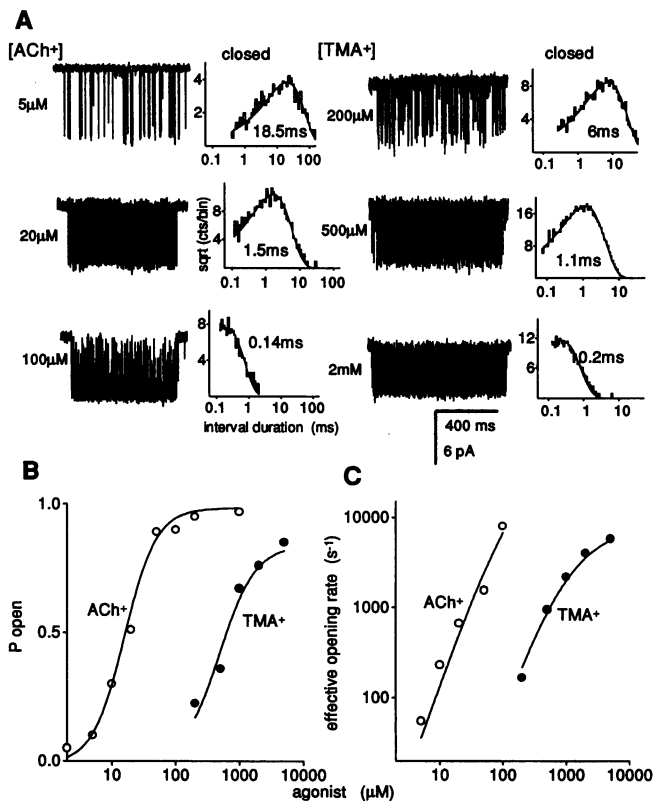


FIGURE 4 Kinetic analysis of adult, wild-type AChR activated by ACh^+ and TMA^+ . (A) Example clusters and closed interval duration histograms. The time constant of the slowest component in the intracuster closed interval duration distribution is given (115 mM NaCl , -100 mV). (B) P_{open} versus [agonist]. The EC_{50} values are $16 \mu\text{M}$ for ACh^+ and $586 \mu\text{M}$ for TMA^+ . Equilibrium constants obtained by fitting the dose-response curves are given in Table 1. Each symbol is one patch. For TMA^+ , the number of clusters per patch was 8 to 46 (mean = 24), and the average SD of the P_{open} was 0.06. (C) The effective opening rate versus [agonist]. For TMA^+ , the error limits of the time constant (the slowest component of intracuster closed intervals) were 4–7% of the optima. In B and C the solid lines are computed from rate constants estimated by single-channel kinetic analysis (Table 2). The P_{open} and opening rate curves for TMA^+ are right-shifted because TMA^+ binds to receptors ~ 11 times more slowly than ACh^+ , and because TMA^+ -activated receptors open ~ 7 times more slowly than ACh^+ -activated receptors.

TABLE 3 Selectivity of the AChR transmitter binding site for monovalent cations

	K_d (mM)	$\Delta\Delta G$ (kcal/mol)
Na^+	151.0	—
K^+	92.0	-0.28
Cs^+	38.0	-0.82
TMA^+	0.47	-3.71
ACh^+	0.06	-4.73

The K_d values are the equilibrium dissociation constants in pure water obtained from single-channel analyses. The $\Delta\Delta G$ values are relative to Na^+ . Estimates of the equilibrium dissociation constants for Na^+ and Cs^+ were obtained from Eq. 3 ($k_+^* = 2.6 \times 10^8 \text{ M}^{-1} \text{ s}^{-1}$), and the k_+ values were estimated by single-channel kinetic modeling (Table 2). The K_d s for ACh^+ and TMA^+ are different from the values given in Tables 1 and 2 because they have been corrected for competitive inhibition by ions.

arise from alterations in ionic competition as well as from alterations of agonist-receptor interactions. Finally, we note that most, if not all, neurotransmitters have an amino moiety that is cationic at physiological pH. It is thus possible that a similar, or more aggressive, competition between transmitter and ion takes place at other receptors (Smith and McBurney, 1989; Hirano et al., 1987). At some synapses changes in the ionic composition of the synaptic gap (for example, an increase in extracellular $[K^+]$) may modulate the amplitude and kinetics of the synaptic response.

We thank Steven Sine for kindly providing the clones of the α D200N and α G153S mutants, and for comments on the manuscript. We thank Karen Lau for technical assistance.

This work was supported by the National Institutes of Health (NS23513) and the Muscular Dystrophy Association.

REFERENCES

- Adams, D. J., T. M. Dwyer, and B. Hille. 1980. The permeability of endplate channels to monovalent and divalent metal cations. *J. Gen. Physiol.* 75:493–510.
- Auerbach, A. 1993. A statistical analysis of acetylcholine receptor activation in *Xenopus* myocytes: stepwise vs concerted models of gating. *J. Physiol. (Lond.)* 461:339–378.
- Ausubel, F. M., R. Brent, R. E. Kingston, D. D. Moore, J. G. Seidman, J. A. Smith, and K. Struhl. 1992. Short Protocols in Molecular Biology. John Wiley and Sons, New York.
- Aylwin, M. L., and M. M. White. 1994. Gating properties of mutant acetylcholine receptors. *Mol. Pharmacol.* 46:1149–1155.
- Changeaux, J.-P., J.-L. Galzi, A. Devillers-Thierry, and D. Bertrand. 1992. The functional architecture of the acetylcholine nicotinic receptor explored by affinity labeling and site-directed mutagenesis. *Q. Rev. Biophys.* 25:395–432.
- Chen, J., Y. Zhang, G. Akk, S. Sine, and A. Auerbach. 1995. Activation kinetics of recombinant mouse nicotinic acetylcholine receptors: mutations of α -subunit tyrosine 190 affect both binding and gating. *Biophys. J.* 69:849–859.
- Colquhoun, D., and A. G. Hawkes. 1977. Relaxation and fluctuations of membrane currents that flow through drug-operated channels. *Proc. R. Soc. Lond. B.* 199:231–262.
- Colquhoun, D., and F. J. Sigworth. 1983. Fitting and statistical analysis of single-channel records. In *Single-Channel Recording*. B. Sakmann and E. Neher, editors. 191–264.
- del Castillo, J., and Katz, B. 1957. Interaction at endplate receptors between different choline derivatives. *Proc. R. Soc. Lond. B.* 146:369–381.
- Gage, P. W., and D. Van Helden. 1979. Effects of permeant monovalent cations on end-plate channels. *J. Physiol. (Lond.)* 288:509–528.
- Gibson, R. E., S. Juni, and R. O'Brien. 1977. Monovalent ion effects on acetylcholine receptor from *Torpedo californica*. *Arch. Biochem. Biophys.* 179:183–188.
- Hamill, O. P., A. Marty, E. Neher, B. Sakmann, and F. J. Sigworth. 1981. Improved patch-clamp techniques for high-resolution current recording from cells and cell-free membrane patches. *Pflugers Arch.* 391:85–100.
- Hille, B. 1992. *Ionic Channels of Excitable Membranes*. Sinauer Associates, Sunderland, MA.
- Hirano, T., Y. Kidokoro, and H. Ohmori. 1987. Acetylcholine dose-response relation and the effect of cesium ions in the rate adrenal chromaffin cell under voltage clamp. *Pflugers Arch.* 408:401–407.
- Horn, R., and K. Lange. 1993. Estimating kinetic constants from single channel data. *Biophys. J.* 43:207–223.
- Magleby, K. L., and C. F. Stevens. 1972. A quantitative description of end-plate currents. *J. Physiol. (Lond.)* 223:173–197.
- Marshall, C. G., D. Ogden, and D. Colquhoun. 1991. Activation of ion channels in the frog endplate by several analogues of acetylcholine. *J. Physiol. (Lond.)* 433:73–93.
- O'Leary, M. E., and M. M. White. 1992. Mutational analysis of ligand-induced activation of the *Torpedo* acetylcholine receptor. *J. Biol. Chem.* 267:8360–8365.
- Qin, F., A. Auerbach, and F. Sachs. 1996. Estimating single-channel kinetic parameters from idealized patch-clamp data containing missed events. *Biophys. J.* 70:264–280.
- Roux, B., and R. Sauve. 1985. A general solution to the time interval omission problem applied to single channel analysis. *Biophys. J.* 48:149–158.
- Sakmann, B., J. Patlak, and E. Neher. 1980. Single acetylcholine-activated channels show burst-kinetics in presence of desensitizing concentrations of agonist. *Nature.* 286:71–73.
- Sine, S. M. 1993. Molecular dissection of subunit interfaces in the acetylcholine receptor: identification of residues that determine curare selectivity. *Proc. Natl. Acad. Sci USA.* 90:9436–9440.
- Sine, S. M., T. Claudio, and F. J. Sigworth. 1990. Activation of *Torpedo* acetylcholine receptors expressed in mouse fibroblasts. *J. Gen. Physiol.* 96:395–437.
- Sine, S., K. Ohno, C. Bouzat, A. Auerbach, M. Milone, J. N. Pruitt, and A. Engel. 1995. Mutation of the acetylcholine receptor α -subunit causes a congenital myasthenic syndrome by enhancing agonist binding affinity. *Neuron.* 15:229–239.
- Sine, S. M., P. Quiram, F. Papanikolaou, H.-J. Kreienkamp, and P. Taylor. 1994. Conserved tyrosines in the alpha subunit of the nicotinic acetylcholine receptor stabilize quaternary ammonium groups of agonists and curariform antagonists. *J. Biol. Chem.* 269:8808–8816.
- Smith, S. M., and McBurney, R. N. 1989. Caesium ions: a glycine-activated channel agonist in rat spinal cord neurones grown in cell culture. *Br. J. Pharmacol.* 96:940–948.
- Sussman, J. L., M. Harel, F. Frolow, C. Oefner, A. Goldman, L. Toker, and I. Silman. 1991. Atomic structure of acetylcholinesterase from *Torpedo californica*: a prototypic acetylcholine-binding protein. *Science.* 253:872–879.
- Tomaselli, G. F., J. T. McLaughlin, M. E. Jurman, E. Hawrot, and G. Yellen. 1991. Mutations affecting agonist sensitivity of the nicotinic acetylcholine receptor. *Biophys. J.* 60:721–727.
- Unwin, N. 1993. Nicotinic acetylcholine receptor at 9 Å resolution. *J. Mol. Biol.* 229:1101–1124.
- Zhang, Y., J. Chen, and A. Auerbach. 1995. Kinetics of wild-type, embryonic nicotinic acetylcholine receptors activated by acetylcholine, carbamylcholine, and tetramethylammonium. *J. Physiol. (Lond.)* 481:189–206.